

## Visco-Hyperelastic Model for Soft Rubber-like Materials (Model Likat-Hiperkenyal untuk Bahan Lembut seperti Getah)

MOHD AFANDI P. MOHAMMED\*

### ABSTRACT

*This paper investigates the application of visco-hyperelastic model to soft rubberlike material, that is gluten. Gluten is a major protein in wheat flour dough (a mixture of flour and water) which exists as long network fibers and undergo large deformation under uniaxial tension and compression. The visco-hyperelastic model is represented by a combination of the viscoelastic Prony series and the hyperelastic extended tube model. Calibration of the visco-hyperelastic model to gluten tests result suggests that gluten can be modelled as a finite viscoelastic material.*

*Keywords: Extended tube model; gluten; hyperelastic; viscoelastic*

### ABSTRAK

*Kertas ini mengkaji aplikasi model likat-hiperkenyal kepada bahan lembut seperti getah, iaitu gluten. Gluten ialah protein utama di dalam doh gandum (campuran tepung gandum dan air) yang wujud sebagai rangkaian gentian panjang dan melalui pemanjangan oleh tegangan dan mampatan. Model likat-hiperkenyal tersebut diwakili oleh kombinasi likat kenyal siri Prony dan model hiperkenyal lanjutan tiub. Kalibrasi model likat-hiperkenyal kepada data kajian daripada bahan gluten mencadangkan bahawa gluten boleh dimodelkan sebagai bahan likat kenyal terhingga.*

*Kata kunci: Gluten; hiperkenyal; likat kenyal; model lanjutan tiub*

### INTRODUCTION

Food materials like bread dough, gluten, and cheese are shown to behave like rubberlike and strain rate-dependent materials (Charalambides et al. 2006; Goh et al. 2004; Ng & McKinley 2008; Tanner et al. 2008). Rate-dependent materials are also known as viscoelastic materials, whereas rubberlike materials are known as hyperelastic materials. A combination of the viscoelastic and hyperelastic is simply referred to as visco-hyperelastic materials. Constitutive modelling of these materials is performed using finite element (FE) method (Charalambides et al. 2006) in commercially available software such as Abaqus (2009). However, before model with complex geometry is generated in Abaqus, it is suggested that calibration of analytical equations to test results to be performed, which yield the same results as the one in finite element (FE) software. The advantage of using analytical equations for non-linear constitutive models (i.e. visco-hyperelastic model) is that it can be performed using spreadsheet like Microsoft Excel, which has the capability to perform least squares method to optimise material model parameters. Therefore, this paper investigates constitutive modelling of analytical visco-hyperelastic model for soft rubberlike material, i.e. gluten. This is performed by a development of the visco-hyperelastic model, which is introduced through a combination of the viscoelastic Prony series (Kaliske et al. 2001) and the hyperelastic extended tube model (Vilgis et al. 2009). In the next section, derivation of the visco-hyperelastic model will be shown. This is followed

by a discussion on the experimental work of gluten by Mohammed et al. (2011). Finally, calibration of the model to the experimental results of wheat gluten by Mohammed et al. (2011) is shown and discussed.

### METHODS

#### DERIVATION OF VISCO-HYPERELASTIC MODEL

The finite viscoelastic model is discussed as below. The theoretical and experimental behaviours of viscoelastic materials were first established in the 19th century by physicists Maxwell, Boltzmann and Kelvin. Viscoelastic materials can be viewed as having both viscous and elastic properties. Elastic materials stretch and return to their original state instantaneously upon application and removal of stress, respectively. The ratio of stress to strain for an elastic material is defined as elastic modulus. Viscous materials on the other hand change strain in proportion to the time that the stress is applied (Janmey & Schiwa 2008). The ratio of stress to rate of strain is defined as viscosity. Viscoelastic materials can exhibit strain and time dependent behaviour when both viscous and elastic properties are present. The mathematical theory of viscoelasticity is as follows.

Viscoelasticity assumes a homogeneous and isotropic material, as well as separable time and strain dependent material behaviour (Charalambides et al. 2006; Goh et al. 2004; Williams 1980). The relaxation stress under a

step strain loading history can be written as a product of a function of time,  $g(t)$  and a function of strain,  $\sigma_0(\varepsilon)$ :

$$\sigma(\varepsilon, t) = \sigma_0(\varepsilon)g(t). \quad (1)$$

The time function can be represented by the Prony Series (Goh et al. 2004):

$$g(t) = g_\infty + \sum_{i=1}^N g_i \exp\left(-\frac{t}{\xi_i}\right), \quad (2)$$

where  $t$  and  $\xi_i$  are time and relaxation time constants, respectively and  $g_i$  are dimensionless constants. The 1D equivalent of the Prony series in tension consists of a series of Maxwell elements connected in parallel with a spring is shown in Figure 1.

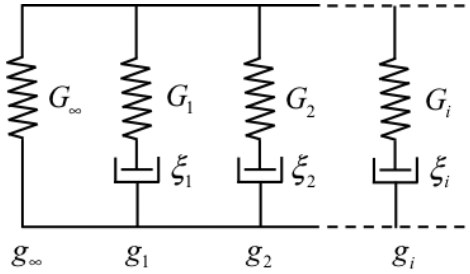


FIGURE 1. The Prony series representation

Each  $g_i$  is defined as:

$$g_i = \frac{G_i}{G_0}, \quad g_\infty = \frac{G_\infty}{G_0}, \quad (3)$$

where  $G_i$  is the modulus of the  $i^{\text{th}}$  spring,  $G_\infty$  is the modulus of the infinite lone spring and  $G_0$  is the instantaneous modulus, given by  $\sum_{i=1}^N G_i + G_\infty = G_0$ . Therefore  $g_i$  is related to  $g_\infty$  through  $\sum_{i=1}^N g_i + g_\infty = 1$ . The function  $\sigma_0(\varepsilon)$  represents the instantaneous stress-strain relationship since and from (1). Note that is the long term or equilibrium stress-strain relationship as  $g(\infty) = g_\infty$  and  $\sigma(\varepsilon, \infty) = g_\infty \sigma_0(\varepsilon)$  from (1). This long term behaviour occurs physically as the dashpots relax the  $i$  springs in Figure 1 and only the  $g_\infty$  spring remains loaded.

Using the Leaderman form of the convolution integral (Williams 1980), the total stress is given by the algebraic sum of the entire past loading history, with each stress component being independent of the loading history. In the limit of continuous strain history, the total stress at time  $t$  is therefore given by (Williams 1980):

$$\sigma(\varepsilon, t) = \int_0^t g(t-s) \frac{d\sigma_0(\varepsilon)}{ds} ds, \quad (4)$$

where  $\sigma_0(\varepsilon)$  is the instantaneous true stress at strain  $\varepsilon$ . The function  $g(t-s)$  is described as:

$$g(t-s) = g_\infty + \sum_{i=1}^N g_i \exp\left(-\frac{t-s}{\xi_i}\right). \quad (5)$$

Therefore (4) becomes:

$$\sigma(t) = \int_0^t \left[ g_\infty + \sum_{i=1}^N g_i \exp\left(-\frac{t-s}{\xi_i}\right) \right] \frac{d\sigma_0(\varepsilon)}{ds} ds. \quad (6)$$

The stress on the left-hand side is expressed in terms of  $t$  only, provided that the strain history  $\varepsilon(t)$  is known (Goh et al. 2004). Equation (6) can be rewritten as:

$$\begin{aligned} \sigma(t) &= g_\infty \sigma_0(t) + \sum_{i=1}^N \int_0^t g_i \exp\left(-\frac{t-s}{\xi_i}\right) \frac{d\sigma_0(s)}{ds} ds \\ &= g_\infty \sigma_0(t) + \sum_{i=1}^N h_i(t) \end{aligned} \quad (7)$$

$$\text{with } h_i(t) = \int_0^t g_i \exp\left(-\frac{t-s}{\xi_i}\right) \frac{d\sigma_0(s)}{ds} ds.$$

The convolution integral in (7) is computed using a numerical algorithm based on finite time increments (Kaliske & Rothert 1997). For a time interval  $(t_n, t_{n+1})$  and time step  $\Delta t = t_{n+1} - t_n$ , the exponential term in the integrand is written as:

$$\exp\left(-\frac{t_{n+1}}{\xi_i}\right) = \exp\left(-\frac{t_n}{\xi_i}\right) \exp\left(-\frac{\Delta t}{\xi_i}\right). \quad (8)$$

The term  $h_i$  at  $t_{n+1}$  can be separated into two components: The first component corresponds to deformation history during period  $0 \leq s \leq t_n$  while the second component corresponds to the period,  $t_n \leq s \leq t_{n+1}$ . Therefore:

$$h_i(t_{n+1}) = g_i \int_0^{t_{n+1}} \exp\left(-\frac{t_{n+1}-s}{\xi_i}\right) \frac{d\sigma_0(s)}{ds} ds, \quad (9)$$

which becomes:

$$\begin{aligned} h_i(t_{n+1}) &= g_i \int_0^{t_n} \exp\left(-\frac{t_{n+1}-s}{\xi_i}\right) \frac{d\sigma_0(s)}{ds} ds \\ &\quad + g_i \int_{t_n}^{t_{n+1}} \exp\left(-\frac{t_{n+1}-s}{\xi_i}\right) \frac{d\sigma_0(s)}{ds} ds. \end{aligned} \quad (10)$$

The first integral above is integrated from 0 to  $t_n$ , which yields:

$$\exp\left(-\frac{\Delta t}{\xi_i}\right) g_i \int_0^{t_n} \exp\left(-\frac{t_n-s}{\xi_i}\right) \frac{d\sigma_0(s)}{ds} ds. \quad (11)$$

The result is included in (7):

$$\begin{aligned} \sigma(t_{n+1}) &= g_\infty \sigma_0(t_{n+1}) \\ &\quad + \sum_{i=1}^N \left[ \exp\left(-\frac{\Delta t}{\xi_i}\right) h_i(t_n) + g_i \int_{t_n}^{t_{n+1}} \exp\left(-\frac{t_{n+1}-s}{\xi_i}\right) \frac{d\sigma_0(s)}{ds} ds \right]. \end{aligned} \quad (12)$$

$\frac{d\sigma_0(s)}{ds}$  in (12) can be expressed in terms of discrete time steps:

$$\frac{d\sigma_0(s)}{ds} = \lim_{\Delta s \rightarrow 0} \frac{\Delta\sigma_0(s)}{\Delta s} = \lim_{\Delta t \rightarrow 0} \frac{\sigma_0^{n+1} - \sigma_0^n}{\Delta t}. \quad (13)$$

Substituting (13) into (12) and performing the last integral in (12) leads to a function for updating the stress  $\sigma(t_{n+1})$  (Goh et al. 2004):

$$\begin{aligned} \sigma(t_{n+1}) = & g_\infty \sigma_0(t_{n+1}) \\ & + \sum_{i=1}^N \left( \exp\left(-\frac{\Delta t}{\xi_i}\right) h_i(t_n) + g_i \frac{1 - \exp\left(-\frac{\Delta t}{\xi_i}\right)}{\frac{\Delta t}{\xi_i}} [\sigma_0(t_{n+1}) - \sigma_0(t_n)] \right). \end{aligned} \quad (14)$$

Equation (14) can be evaluated with various rubberlike (hyperelastic) potentials. The true stress,  $\sigma(t_n)$  used will be discussed later in this section.

It is worth noting that in the newer version of the commercial finite element software, Abaqus version 6.9 (Abaqus 2010), an updated version of viscoelastic model has been introduced to replace the former Abaqus version 6.8 (Abaqus 2009) (14). A modification is performed to (6) as follows:

$$\sigma(t) = \lambda(t) \int_0^t \left[ g_\infty + \sum_{i=1}^N g_i \exp\left(-\frac{t-s}{\xi_i}\right) \right] \frac{dP_0(\varepsilon)}{ds} ds. \quad (15)$$

Notice the difference where  $\sigma_0$  in (6) represents the true stress term, whereas  $P_0$  in (15) represents the nominal stress term. The stretch ratio,  $\lambda(t)$  is introduced in (15) to convert the nominal stress term in the integral into true stress term after integration. True stress and nominal stress are related through:

$$\sigma_0(t_n) = P_0(t_n) \cdot \lambda(t_n). \quad (16)$$

Equation (15) is then evaluated using the same finite time increment algorithm as before, which finally yields:

$$\begin{aligned} \sigma(t_{n+1}) = & g_\infty \sigma_0(t_{n+1}) \\ & + \lambda(t_{n+1}) \sum_{i=1}^N \left( \exp\left(-\frac{\Delta t}{\xi_i}\right) h_i(t_n) + g_i \frac{1 - \exp\left(-\frac{\Delta t}{\xi_i}\right)}{\frac{\Delta t}{\xi_i}} [P_0(t_{n+1}) - P_0(t_n)] \right). \end{aligned} \quad (17)$$

On the other hand, the following form of viscoelastic model can be used:

$$\sigma(t) = \lambda^2(t) \int_0^t \left[ g_\infty + \sum_{i=1}^N g_i \exp\left(-\frac{t-s}{\xi_i}\right) \right] \frac{dS_0(\varepsilon)}{ds} ds, \quad (18)$$

where  $S_0$  in (17) represents the Second Piola Kirchoff stress term, as performed by Kaliske et al. (2001). The stretch ratio,  $\lambda^2(t)$  is introduced in (18) to convert  $S_0$  in the integral into true stress term after integration. True stress and the Second Piola Kirchoff are related through:

$$\sigma_0(t_n) = S_0(t_n) \cdot \lambda^2(t_n). \quad (19)$$

Equation (18) is then evaluated using the same finite time increment algorithm as before, which yields:

$$\begin{aligned} \sigma(t_{n+1}) = & g_\infty \sigma_0(t_{n+1}) \\ & + \lambda^2(t_{n+1}) \sum_{i=1}^N \left( \exp\left(-\frac{\Delta t}{\xi_i}\right) h_i(t_n) + g_i \frac{1 - \exp\left(-\frac{\Delta t}{\xi_i}\right)}{\frac{\Delta t}{\xi_i}} [S_0(t_{n+1}) - S_0(t_n)] \right). \end{aligned} \quad (20)$$

The advantage of using (20) is that the Second Piola Kirchoff stress does not admit a physical interpretation in terms of surface traction as well as having a symmetric tensor function (Holzapfel 2000). This allows a damage function to be included into the finite viscoelastic model, as performed by Kaliske et al. (2001). For details on the derivation of Second Piola Kirchoff, true and nominal stresses using tensor mechanics, please refer to Holzapfel (2000).

The difference between the finite viscoelastic model in Abaqus versions 6.8 and 6.9 (14 and 17) are highlighted in their respective Abaqus theory user manuals (Abaqus 2009; 2010). This has also been discussed theoretically by Ciambella et al. (2009) whose suggested that the finite viscoelastic model in Abaqus version 6.8 (14) cannot describe accurately the 3D FE viscoelastic model at large strain.

The advantage of the analytical equation discussed in this section is that it can be readily fitted to experimental stress-strain data which are measured at known time intervals. The equation offers a very practical method for determining material constants at any deformation history. A spreadsheet can be set up so that the calculations using the analytical equation are matched to the experimental data via a least squares error method.

The true stress,  $\sigma_0(t_n)$  used in the finite viscoelastic model (i.e. (20)) is obtained using the extended tube model. The extended tube model is described by first considering the concept of rubberlike materials. A rubberlike material is defined as an ideally elastic material, but may be subjected to large deformations and still show complete recovery (Ward 1971). The rubber elasticity can be described using the concept of a strain energy function derived from thermodynamic considerations. Different types of strain energy function can be defined, depending on the experimental conditions. Strain energy functions can be described from either a phenomenological or a statistical mechanics. In statistical mechanics, the strain energy function is represented as the Helmholtz free energy of

a molecular network with a Gaussian chain distribution (Treloar 1975). The theory can be described from the First Law of Thermodynamics:

$$dW = dU - dQ, \quad (21)$$

where  $dW$  is work performed on the system by the surroundings,  $dU$  and  $dQ$  are differential change in internal energy and heat, respectively. Under adiabatic conditions,  $dQ = 0$  and  $dW = dU$ . The strain energy function  $W$  for an isotropic incompressible solid undergoing a pure homogeneous deformation is given by (Ward 1971):

$$W = f(I_1, I_2, I_3), \quad (22)$$

where  $f$  is a function of  $I_1$ ,  $I_2$  and  $I_3$ , which are the first, second and third strain invariants, respectively, expressed as:  $I_1 = \lambda_1^2 + \lambda_2^2 + \lambda_3^2$ ,  $I_2 = \lambda_1^2\lambda_2^2 + \lambda_2^2\lambda_3^2 + \lambda_3^2\lambda_1^2$  and  $I_3 = \lambda_1\lambda_2\lambda_3$ . The third strain invariant,  $I_3$ , is assumed to be unity due to the assumption of incompressibility.  $\lambda_1$ ,  $\lambda_2$  and  $\lambda_3$  are the stretch ratios in the three principal axis, which are defined for uniaxial deformation (i.e. uniaxial compression and tension) as:

$$\lambda_1 = \lambda, \lambda_2 = \lambda_3 = \frac{1}{\sqrt{\lambda}}, \quad (23)$$

where  $\lambda$  is the stretch ratio in the direction of the applied load. The stretch ratio,  $\lambda$  is described as:  $\lambda = (l/l_0)$ , where  $l$  and  $l_0$  are the current and original heights, respectively. The current height,  $l_0$  is defined as:  $(l = l_0 + \delta)$ , where deformation,  $\delta$  is defined in tension  $\delta > 0$  and  $\delta < 0$  in compression.  $I_1$ ,  $I_2$  and  $I_3$  in the case of uniaxial deformation can be described as:

$$I_1 = \lambda^2 + 2\lambda^{-1}, \quad I_2 = 2\lambda + \lambda^{-2}, \quad I_3 = 1. \quad (24)$$

Note that  $I_3 = 1$  in (24) indicates incompressibility assumption. For uniaxial tension and uniaxial compression, the true stress used in (14) is given as a function of  $\lambda$ :

$$\sigma_0(\lambda) = \frac{\partial W}{\partial \lambda} \lambda. \quad (25)$$

Examples of the strain energy function,  $W$  or hyperelastic models developed using statistical mechanics includes the van der Waals rubber model (Kilian 1982), Arruda-Boyce model (1993) and Edwards-Vilgis model (Edwards & Vilgis 1986).

This work therefore considered the statistical mechanics approach, in particular the extended tube model by Kluppel and Schramm (2000) and Vilgis et al. (2009). The model can be described using the analogy a network chain in a virtual tube. The tube is allowed to expand and contracts, where the tube movement is described using a Gaussian distribution function. The strain energy function for the extended tube model can be defined as follows (Kluppel & Schramm 2000).

$$W = W_c + W_e, \quad (26)$$

where  $W_c$  is the energy related to cross-link of network and  $W_e$  is the energy related to topological tube-like constraint. Equation (26) then becomes (Kluppel et al. 2001):

$$W = G_c \left( \sum_{\mu=1}^3 \lambda_{\mu}^2 - 3 \right) + 2G_e \left( \sum_{\mu=1}^3 \lambda_{\mu}^{-1} - 3 \right). \quad (27)$$

The moduli,  $G_c$  and  $G_e$  are elastic modulus and 'entanglement' modulus, respectively. The elastic modulus increases as the density of network junctions increases, whereas the 'entanglement' modulus is proportional to the entanglement density of the rubber network. To improve the first term in (27), Kluppel et al. (2001) suggested the path integral approach for the network rubber by Edwards and Vilgis (1986), which is expressed as:

$$\psi[R(s)] = \text{const} \times \exp \left( -\frac{3}{2I_s} \int_0^L ds \left( \frac{(R'(s))^2}{1-(R'(s))^2} + \gamma (R''(s))^2 \right) \right), \quad (28)$$

where  $I_s$  and  $L$  are the Kuhn length and the total length of polymer chain, respectively and  $\text{const}$  is a constant. The Kuhn length describes freely jointed segments of the polymer chain.  $R$  is described as a locus in space or coordinate,  $S$  of a long polymer chain (Edwards & Vilgis 1986), where the mean value of  $\langle R'(s) \rangle$ , is described as:

$$\langle R'(s) \rangle = \frac{T_e}{n_e}, \quad (29)$$

whereas  $R'(s)$  is described as  $R'(s) \equiv \partial R(s)/\partial s^2$ . The parameter,  $T_e$  represents the trapping factor with the following constraint:  $(0 < T_e < 1)$ , which characterises the portion of elastically active entanglements of rubber chains. The parameter,  $n_e$  on the other hand is the number of statistical chains segments between two successive entanglements, which increases as the crosslink density increases. A modification was performed by Kluppel et al. (2001) using (27), (28) and (29), which yields:

$$W = \frac{G_c}{2} \left\{ \frac{\left( \sum_{\mu=1}^3 \lambda_{\mu}^2 - 3 \right) \left( 1 - \frac{T_e}{n_e} \right)}{1 - \frac{T_e}{n_e} \left( \sum_{\mu=1}^3 \lambda_{\mu}^2 - 3 \right)} + \ln \left[ 1 - \frac{T_e}{n_e} \left( \sum_{\mu=1}^3 \lambda_{\mu}^2 - 3 \right) \right] \right\} + 2G_e \left( \sum_{\mu=1}^3 \lambda_{\mu}^{-1} - 3 \right), \quad (30)$$

where the first and second terms in (30) is related to  $W_c$  and  $W_e$  in (26), respectively. Note that in the limit of  $n_e \rightarrow \infty$ , (30) will becomes (27).

Finally, the true stress for (30) is obtained using (25) and (30):

$$\sigma = G_c (\lambda^2 - \lambda^{-1}) \left\{ \frac{1 - \frac{T_e}{n_e}}{1 - \frac{T_e}{n_e} \left( \lambda^2 - \frac{2}{\lambda} - 3 \right)^2} - \frac{\frac{T_e}{n_e}}{1 - \frac{T_e}{n_e} \left( \lambda^2 - \frac{2}{\lambda} - 3 \right)} \right\} + 2G_e (\lambda^{1/2} - \lambda^{-1}). \quad (31)$$

Note that several polymer tube models are available in literature, for example the Pom-Pom model (McLeish & Larson 1998), the Doi-Edwards model (Doi & Edwards 1986) and the extended tube model by Kaliske et al. (2001).

#### EXPERIMENTAL WORK ON GLUTEN

Gluten is a major protein in wheat flour dough (a mixture of flour and water), which exists as long network fibers (Singh & MacRitchie 2001). This enables gluten to undergo large deformation under uniaxial tension and compression (Charalambides et al. 2006; Tanner et al. 2008). By using the polymer network theory, Singh and MacRitchie (2001) suggested that gluten can be treated as a rubber-like material. On the other hand, gluten has been shown to behave like a viscoelastic material by previous researchers (Ng & McKinley 2008; Ng et al. 2011; Uthayakumaran 2002) based on stress relaxation rheometry tests. To investigate the behaviour of gluten discussed before, the experimental results of gluten are shown in Figure 2, which were obtained from Mohammed et al. (2011).

The results consist of uniaxial compression, uniaxial tension, compression relaxation and cyclic compression tests. The uniaxial tension tests were performed by clamping both ends of a sample and pulling them in opposite directions at a fixed rate using a testing machine (i.e. Universal Testing Machine). The load direction in the tensile test is opposite to the load direction in the uniaxial compression test. A stress relaxation test was conducted in compression mode, where a specimen was compressed to a required strain and held fixed for a period of time while the stress decay was measured. Cyclic compression tests were performed by loading and unloading a sample under compression mode at the same strain rate. The reloading curve for the cyclic compression tests was activated once the stress in the unloading curve becomes zero. Details on the experimental procedures involved are discussed in Mohammed et al. (2011, 2013). It can be seen in Figure 2 that gluten shows rubberlike (strain hardening) behaviour under uniaxial tension. On the other hand, the stress relaxation test results and different stress-strain curve under different strain rate suggests viscoelastic behaviour of gluten. Therefore a combination of viscoelastic and hyperelastic model (visco-hyperelastic model) is believed to represent the mechanical behaviour of gluten. This will be investigated further in the next section using the visco-hyperelastic model.

## RESULTS AND DISCUSSION

### CALIBRATION OF VISCO-HYPERELASTIC MODEL TO GLUTEN TESTS RESULTS

In order to illustrate the application of the visco-hyperelastic model discussed in the previous section, calibration of the model (20) and (31) was performed and compared to the experimental results of gluten by Mohammed et al. (2011) (Figure 2). Calculation of the equations was performed using Microsoft Excel spreadsheet, where the analytical equations were matched to the experimental data via a least squares method (Goh et al. 2004).

The parameters which give the best fit to the experimental results in Figure 2 are shown in Table 1. It can be seen that the Prony series constants reduced from 0.5 at 0.1 s to 0.045 at 1000 s, which indicates the stress relaxed over time at strain -1.

Noticed that the model agrees reasonable well to the experimental results except for the tension results (Figure 2(b)) for strain larger than 0.7. This indicates that further work is needed to ensure that the model parameters represent the physical behaviour of the material tested. To achieve this, Vilgis et al. (2009) suggested that in addition to stress-strain measurements which yields the modulus and shape of the stress-strain curve, investigation on the neutron scattering of biopolymer networks (i.e. gluten) can be conducted, which would corresponds to the probability distribution of the networks. It is worth noting that the microstructure networks of gluten consist of glutenin and gliadin (Edwards et al. 2003), where the exact contribution of these constituents toward elasticity of gluten is not clearly identified. On the other hand, dynamic mechanical measurements of gluten can be performed using the rheometers, after which unique viscoelastic material parameters for gluten can be determined using the critical gel Lodge-rubberlike model by Ng and McKinley (2008) and Ng et al. (2011).

Finally, further work is suggested to investigate the hysteresis and partial recovery of gluten shown in Figure 2(d), where the gluten unloading stress-strain curve does not recover back to zero when the stress is zero. It is possible that this could be due to the gluten networks being damaged from stretching or compression under large deformation. This could be investigated further using Cryogenic Scanning Electron Microscope (Kontogiorgos & Goff 2006). Discussion on the theory of gluten extensibility is provided by Singh and MacRitchie (2001).

## CONCLUSION

Constitutive modelling of analytical visco-hyperelastic model for soft rubberlike material, i.e. gluten was performed. The mathematical derivation of the visco-hyperelastic model was shown, which consists of a

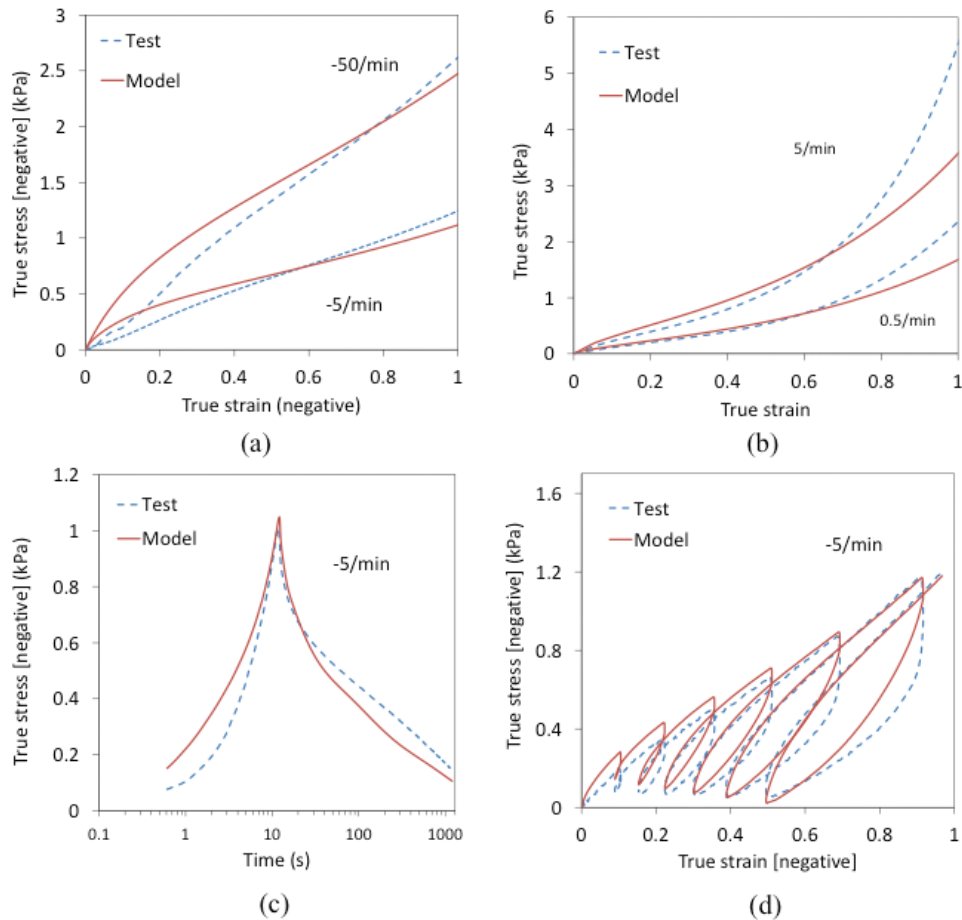


FIGURE 2. Calibration of the visco-hyperelastic model to gluten test results under (a) uniaxial compression, (b) uniaxial tension, (c) compression relaxation at strain -1 and (d) cyclic compression

TABLE 1. Parameters used for the visco-hyperelastic model

| Extended tube model |             |        |       | Prony series constants |     |     |     |      |       |          |
|---------------------|-------------|--------|-------|------------------------|-----|-----|-----|------|-------|----------|
| $G_e$ (kPa)         | $G_c$ (kPa) | $T_e$  | $n_e$ | $i$                    | 1   | 2   | 3   | 4    | 5     | $\infty$ |
| 0.001               | 2.3         | 0.0001 | 10    | $\xi_i$                | 0.1 | 1   | 10  | 100  | 1000  |          |
|                     |             |        |       | (s)                    |     |     |     |      |       |          |
|                     |             |        |       | $g_i$                  | 0.5 | 0.3 | 0.1 | 0.05 | 0.045 | 0.005    |

combination of the viscoelastic Prony series and the hyperelastic extended tube model. The model was calibrated to the gluten tests results. The model agrees reasonably well to the experimental results, except for the tension results for strain larger than 0.7. This suggests that a detailed physical and rheological study is needed to represent a physical behaviour of the gluten tested.

#### REFERENCES

- Abaqus's User Manual ver. 6.8. 2009. Hibbitt Karlsson and Sorensen, Providence, USA.
- Abaqus's User Manual ver. 6.9. 2010. Hibbitt Karlsson and Sorensen, Providence, USA.
- Arruda, E.M. & Boyce, M.C. 1993. A three-dimensional constitutive model for the large stretch behaviour of rubber elastic materials. *J. Mech Phys. Solids*. 41(2): 389-412.
- Ciambella, J., Destrade, M. & Ogden, R.W. 2009. On the Abaqus FEA model of finite viscoelasticity. *Rubber Chem. Tech.* 82(24): 184-193.
- Charalambides, M.N., Wanigasooria, L., Williams, J.G., Goh, S.M. & Chakrabarti, S. 2006. Large deformation extensional rheology of bread dough. *Rheol. Acta* 46: 239-248.
- Doi, M. & Edwards, S.F. 1986. *The Theory of Polymer Dynamics*. Oxford, UK: Oxford University Press.
- Edwards, S.F. & Vilgis, T. 1986. The effect of entanglements in rubber elasticity. *Polymer* 27: 483-492.
- Edwards, N.M., Mulvaney, S.J., Scanlon, M.G. & Dexter, J.E. 2003. Role of gluten and its components in determining

- durum semolina dough viscoelastic properties. *Cereal Chem.* 6: 755-763.
- Goh, S.M., Charalambides, M.N. & Williams, J.G. 2004. Determination of the constitutive constants of non-linear viscoelastic materials. *Mech. Time-Depend. Mate.* 8: 255-268.
- Holzappel, G.A. 2000. *Nonlinear Solid Mechanics: A Continuum Approach for Engineering*. UK: John Wiley and Sons.
- Janmey, P.A. & Schiwa, M. 2008. Rheology. *Current Biology* 18(15): R639-R641.
- Kaliske, M. & Rothert, H. 1997. Formulation and implementation of three-dimensional viscoelasticity at small and finite strains. *Comput. Mech.* 19: 228-239.
- Kaliske, M., Nasdala, L. & Rothert, H. 2001. On damage modelling for elastic and viscoelastic materials at large strain. *Computers Struct.* 79: 2133-2141.
- Kilian, H.G. 1982. Thermo-elasticity of network. *Coll. Polym. Sci.* 260: 895-910.
- Kluppel, M. & Schramm, J. 2000. A generalized tube model of rubber elasticity and stress softening of filler reinforced elastomer systems. *Macromol. Theory Simul.* 9: 742-754.
- Kluppel, M., Menge, H., Schimdt, H., Schneider, H. & Schuster, R.H. 2001. Influence of preparation conditions on network parameters of sulfur-cured natural rubber. *Macromolecules* 34: 8107-8116.
- Kontogiorgos, V. & Goff, H.D. 2006. Calorimetric and microstructural investigation of frozen hydrated gluten. *Food Biophys.* 1: 202-215.
- McLeish, T.C.B. & Larson, R.G. 1998. Molecular constitutive equations for a class of branched polymers: The Pom-Pom model. *J. Rheol.* 42(1): 81-110.
- Mohammed, M.A.P., Tarleton, E., Charalambides, M.N. & Williams, J.G. 2011. A composite model for wheat flour dough under large deformation. *Procedia Food Sci.* 1: 492-498.
- Mohammed, M.A.P., Tarleton, E., Charalambides, M.N. & Williams, J.G. 2013. Mechanical characterization and micromechanical modeling of bread dough. *J. Rheol.* 57(1): 249-272.
- Ng, T.S.K. & McKinley, G.H. 2008. Power law gels at finite strains: The nonlinear rheology of gluten gels. *J. Rheol.* 52(2): 419-449.
- Ng, T.S.K., McKinley, G.H. & Ewoldt, R.H. 2011. Large amplitude oscillatory shear flow of gluten dough: A model power-law gel. *J. Rheol.* 55(3): 627-654.
- Singh, H. & MacRitchie, F. 2001. Application of polymer science to properties of gluten. *J. Cereal Sci.* 33: 231-243.
- Tanner, R.I., Dai, S.C. & Qi, F. 2008. Bread dough rheology and recoil: 1. Rheology. *J. Non-Newton. Fluid Mech.* 148: 33-40.
- Treloar, L.R.G. 1975. *The Physics of Rubber Elasticity*. Oxford, UK: Clarendon Press.
- Uthayakumaran, S., Newberry, M., Phan-Thien, N. & Tanner, R. 2002. Small and large strain rheology of wheat gluten. *Rheol. Acta* 41: 162-172.
- Vilgis, T.A., Heinrich, G. & Kluppel, M. 2009. *Reinforcement of Polymer Nano-composite: Theory, Experiments and Applications*. Cambridge, UK: Cambridge University Press.
- Ward, I.M. 1971. *Mechanical Properties of Solid Polymers*. 2nd ed. UK: Wiley-Interscience Publication.
- Williams, J.G. 1980. *Stress Analysis of Polymers*. London, UK: John Wiley.

Department of Process and Food Engineering  
Universiti Putra Malaysia  
43400 Serdang, Selangor  
Malaysia

\*Corresponding author; email: afandi@eng.upm.edu.my

Received: 6 June 2013

Accepted: 8 July 2013